Decay enhancement of self-trapped excitons at high density and low temperature in an ion-irradiated BaF_2 single crystal

Kazuie Kimura and Wan Hong
The Institute of Physical and Chemical Research (RIKEN), Hirosawa 2-1 Wako-shi, Saitama 351, Japan
(Received 16 June 1997; revised manuscript received 12 March 1998)

The decay of the luminescence due to self-trapped excitons (STE) induced by ion irradiation of a BaF_2 single crystal has been measured. It is shown that the decay of STE created by ion irradiation is much faster than those created by photon and electron irradiation; such decay enhancement is further increased with increasing projectile-ion mass and with decreasing temperature. These results are explained in terms of the effect of high-density excitation by ion irradiation. A competition kinetics between the spontaneous decay and the decay through a nonradiative exchange interaction can simulate the decay curves well. Both effects of excitation density and of temperature attain an ultimate decay time of 150 ps. This may suggest that interaction between the precursors of STE's, such as free excitons, plays a main role in incipient tracks. [S0163-1829(98)08533-6]

I. INTRODUCTION

We have been studying the primary ion-track effect in condensed insulators. Generally, in a time range of subpico- or picoseconds after the primary ion collision, the track contains excited states of the outermost-shell electrons at extremely high density. Energetic ions ionize condensed matter at high density along their tracks, as understood from the large deposition energy, which can be as large as 1000 eV/Å. A major part of the holes and electrons ejected recombine to form excited states or excitons. The outermost-shell holes, which are produced with a much larger probability than the inner-shell holes, form the outermost-shell excitons. Furthermore, the inner-shell holes, too, can be fed to the outermost-shell excitons, because they can be converted into outer-shell holes by the Auger process, and cascades of this process result in the outermost-shell excitons. Therefore, the outermost-shell excitons will be generated at extremely high density along the track, and a ''track effect'' may result as a consequence of exciton-exciton interaction. The high-density excitation is characteristic of ion irradiation, and one may expect the ion irradiation to be a unique method to create excitons at high density especially in a crystal with a large band gap such as alkali or alkaline-earth halides, for which synchrotron radiation, electrons, or laser light is yet insufficient in the intensity or the excitation energy to achieve this. It may be imagined that there must occur a drastic interaction between the excitons in the ion tracks. In order to study the track effect, we have developed luminescence-decay measurement techniques with a resolution of 100 ps and high sensitivity.

Photon and electron irradiation of a BaF_2 single crystal induces luminescence bands with peaks at 220 and 300–310 nm. The 220-nm band found recently was assigned to a transition of a valence electron to an outermost inner-shell hole of BaF_2, Ba^{3+}, and named Auger-free luminescence (AFL).[1–3] AFL is a type of luminescence and is characterized by a decay time as short as 800 ps. Studies on the 300–310 nm band have a longer history not only for BaF_2 but also for other alkaline-earth halides such as CaF_2 and SrF_2, and this band was assigned to self-trapped exciton (STE) luminescence by studies using similar methods for alkali halides.[4,5] Its decay curve was not a simple exponential and was dependent on temperature. In addition, a time-retarded peak was observed at few tens of ns after the incidence of the excitation pulse by recent pulsed synchrotron radiation[6] or by picosecond pulsed electron irradiation[7] at room temperature. The decay curve after the peak was approximated to the exponential with a decay time of about 600 ns tentatively.

The ion irradiation gives AFL also, although it cannot be recognized by the usual time-integration-type luminescence spectrum, which was reported previously.[8] The decay of ion-induced AFL was not exponential, it was dependent on ion mass or the density of excitation, and was much faster than that induced by photon irradiation. The results could be explained by the recombination of dense free electrons with core holes of Ba in competition with AFL in the track. This mechanism does not involve direct interaction among core holes, since core holes are screened by valence electrons and their collisions caused by the diffusion are negligible, especially in a short time range within 100 ps.

We found also that the ion-induced STE decays much faster than the spontaneous decay observed by photon irradiation.[9(c)] This may be ascribed to the track effect on the STE. In this report, further detailed decay of the STE was measured using a fast measurement technique. Dramatic decay enhancement was observed in the initial stage of the decay with increasing excitation density and decreasing temperature. It will be attempted to explain the results by kinetics.

II. EXPERIMENT

In order to measure a luminescence decay with high resolution, we have developed a device named SISP (single-ion hitting single photon counting).[8,9] A recent SISP is basically the same as the one illustrated in Ref. 9(d). The principle of SISP is to measure the time correlation between the instants

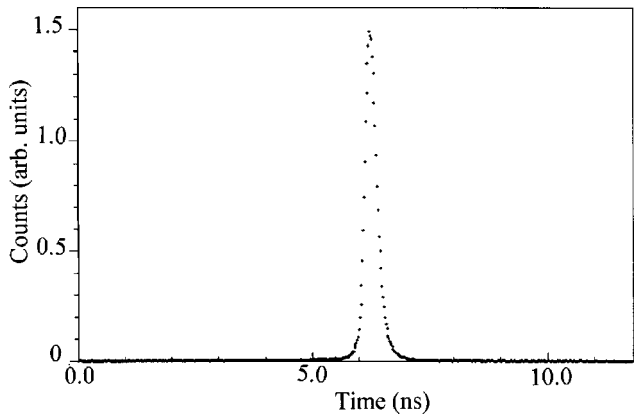

FIG. 1. A time profile in the case where both start and stop pulses were given by FASD's.

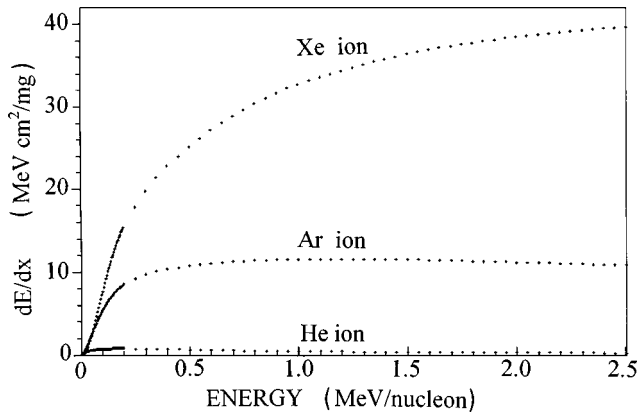

FIG. 2. Stopping power in BaF_2. Calculations were made according to Ref. 2.

of hitting of a single ion to a target and counting of a single photon using a time-to-amplitude converter (TAC) and an analog-to-digital convertor. A single-ion hit is equivalent to an excitation pulse with a negligibly short width. To obtain the single-ion hitting condition or exclude pileup, the ion current of an accelerator was decreased to a rate of about one ion hit per 3000 bunches. A stop pulse for the TAC was provided by a FASD (fast secondary electron detector), which was composed of an 10 μg/cm^2 carbon foil and tandem microchannel plates (MCP) and placed at 45 mm before a target in a cryostat. At present, the distance between the carbon foil and MCP was shortened to 2.7 mm. This resulted in a decrease in the accelerating potential, which excluded accidental electric discharge. The time resolution of the FASD was about 15 ps if it is defined as a root of the full width at half maximum of a histogram measured using two FASD's positioned in series. A result of the measurements is shown in Fig. 1. The start pulse was generated by a MCP-mounted photomultiplier, model R2809u or R3809u from Hamamatsu Photonics. The time resolution of the full system of the SISP was about 100 ps. The luminescence was monochromated by a 25-cm grazing monochromator from Ritsu Ltd. A time-integrated luminescence spectrum was measured by a intensified CCD camera (SMA) from Princeton Instruments Inc.

Projectile ions were accelerated by the heavy-ion LINAC by our institute (RILAC) and collimated to 0.7×0.7 mm^2 by slits made of well polished stainless-steel poles instead of using knife edges. Ions with the same incident velocity were irradiated by using the energies of 2.0 MeV/nucleon for He, N, Ar, Kr ions except for 1.5 MeV/nucleon for Xe ions, in order to compare the effect by different ions meaningfully as possible (see Sec. III b). Ions of these energies are close to their maximum stopping powers[10] (see Fig. 2). The stopping power exhausted in inelastic (electronic) collisions may be estimated more than 99.9% of the total. In the case of the decay measurements of wider time ranges than a few hundred ns beam trains were kicked out electrically, with keeping the condition of single hit, in order that the intervals of ions were not shorter than 20 μs, which excluded pileup.

It should be noted that one output pulse from the TAC corresponds to a single event in a single-ion track. The amount of color centers produced by ion irradiation (less than 10^9 ions) was too small to affect the intensity of luminescence through self-absorption by the centers, which was ascertained by the absorption measurement of the irradiated samples.

A single crystal of BaF_2, provided by Horiba Ltd. was cleaved to plates of $6\times10\times0.5$ mm^3, and a plate was mounted to a holder which can slide the sample up and down in a cold chamber of a cryostat. The cryostat was a modified Oxford model CF200. Cooling of a sample was performed not only by a heat contact but also by He gas at a few tens of Torr in a cold chamber. The sample plate was set at 45° to the ion beams, and luminescence was measured in a direction perpendicular to the ion beams. Neither a change in the cleaving face, (111) or (110), or rotation of sample caused a change in the spectra, within experimental error.

III. RESULTS

A. STE decay curves by photon, electron, and ion irradiation

Figure 3 shows time-resolved and time-integrated luminescence spectra of ion-irradiated BaF_2 single crystals at room temperature, which were measured by a SISP and SMA, respectively. At an initial stage near time 0, there are two bands peaked at 5.6 eV (220 nm) and 4.1 eV (300 nm). The 220-nm band can be assigned to AFL. It disappeared in about 1 ns, as reported already.[8] After 1 ns, only a 300-nm band remained and no significant shift of the peak was rec-

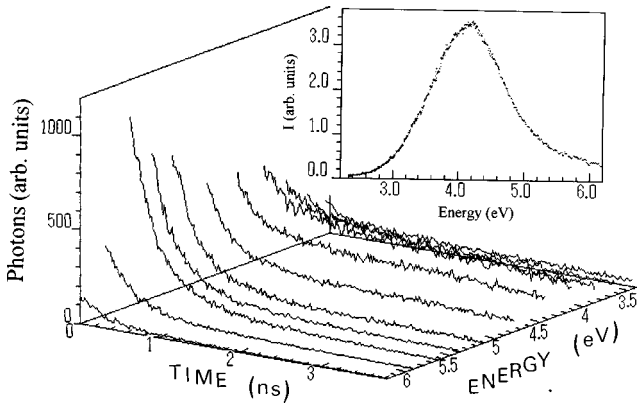

FIG. 3. Time-resolved and time-integrated luminescence spectra of 2.0 MeV/nucleon N-ion irradiated BaF_2 at room temperature. Inset: Time-integrated luminescence spectra.

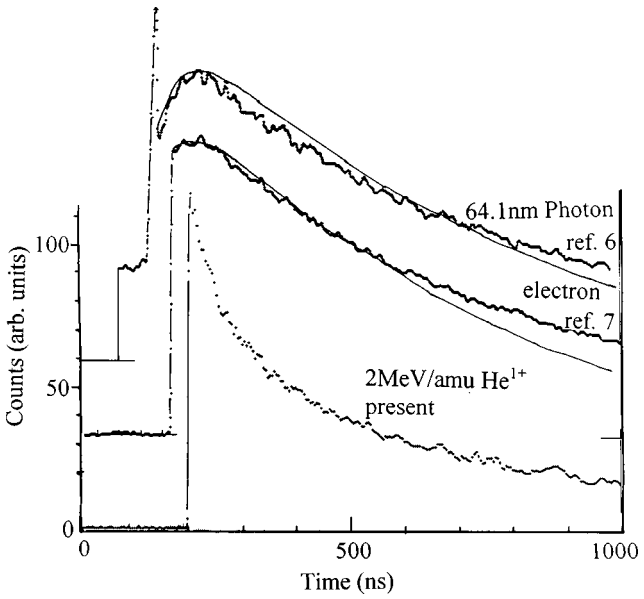

FIG. 4. Decay curves of STE luminescence in BaF_2 irradiated by 64.1 nm photons (Ref. 6), 28 MeV electrons (Ref. 7), and 2 MeV/nucleon He^{1+} ions at room temperature. Thin solid lines stand for theoretical decay curves calculated by Eq. (4).

ognized throughout the time-resolved and time-integrated spectra. Compared with results in the case of photon and electron irradiation,[3–6] this band can be assigned to self-trapped exciton (STE) luminescence.

The decay curve obtained by ion irradiation is considerably different from those obtained by photon and electron irradiation. Figure 4 shows decay curves at the peak wavelength produced by 2.0-MeV/nucleon He ions, 64.1-nm photon,[6] and 28-MeV electrons[7] at room temperature; the initial spike seen in case of photon irradiation is considered to be due to the stray light of exciting pulse of the synchrotron radiation. The decay curves by photon or electron irradiation are characterized by a time-retarded peak, i.e., the time-retarded growth of STE's. The retardation times from the incidence of the irradiation up to the peak can be read to be about 83 and 44 ns for photon and electron irradiation, respectively. These curves were measured using pulsed light of width 130 ps from synchrotron radiation[6] and using a 10-ps electron pulse.[7] The time-retarded peak seen in Fig. 4 is substantial but can not be ascribed to a poor time resolution of the measurement system.

Thermostimulated formation of STE's has been observed after irradiation.[4,6] The thermoluminescence spectrum had a peak near 300 nm at room temperature although the peak wavelength and its intensity are dependent on temperature; the peak shifts from 300 to 310 nm with decreasing temperature. This luminescence was assigned to STE's regenerated by the recombination between the color centers of F and H pairs; actually it may be necessary to take account of V_k centers in addition to H centers analogous to the case of alkali halides. The result[6] that thermoluminescence rises from near 30 K (towards the first small peak at 40 K) suggests that the centers are immobile at lower temperature than 30 K or that, at higher temperature than this, they are mobile to be recombined even at significantly low temperature. The fact[11] that the yield of damage in irradiated BaF_2 is less than those for alkali halides may be a result of the recombination of mobile color centers. Thus, when the STE decay is observed at higher temperature than 30 K, the decay process includes the time-retarded regeneration by the F and H recombination in addition to the pure decay processes. It will be shown by the simulation in the section of discussion that the appearance of the time-retarded peak may be caused by this competition.

In contrast, the decay for 2-MeV/nucleon He-ion irradiation had no time-retarded peak. Furthermore, the decay at the initial stage was much more rapid than the other two. The curvature at the initial stage suggests a decay process quite different from those in the cases of photon and electron irradiation. Also, considering the smooth and continuous curvature of the decay curve, the curve cannot be ascribed to the simple superposition of fast and slow exponentials but may be instead a single function. The difference between electron or photon irradiation and ion irradiation is in their density of deposition energy, in other words, in linear energy transfer (LET) or excitation density which we use often. LET is defined as the incident energy divided by the range of ions. As stated in the Introduction, LET given by ion irradiation is much larger than those by electron and photon irradiation, and hence the former irradiation can form both F-H centers and STE's much more densely than the latter. This can be expected to cause the difference in the decay of the STE between both irradiation. However, the decay curve after 600 ns has curvature similar to those of the photon and electron irradiation. This seems to show that the density effect disappears with the passage of time.

B. LET-enhanced STE decay

Let us show the LET dependence of the decay by using ions having larger LET than that of He. To compare reasonably the effects among various ions with different mass, the ion velocities were equalized to the same velocity of 1×10^7 m/s (corresponds to 2.0 MeV/nucleon), except that the Xe ions corresponded to 1.56 MeV/nucleon. Ions with equal velocities induce a close effect in the primary collision except for the secondary effect such as the effect of the excitation density, since the stopping power, the track radius, and the charge exchange are closely related with the ion velocity. Furthermore, the value of 2.0 MeV/nucleon is due to the energy near the maximum stopping power. Below this ion energy, the energy percent for producing energetic γ rays which can form the hollow part of the track becomes smaller than about 10% of the total deposition energy.[12–14] As a result, we observe predominantly the effect in core parts of tracks of which the sizes are not so different by the difference of ions.

Now, Figs. 5(a) and 5(b) show decay curves of STE luminescence produced by He, N, Ar, and Xe ions at room temperature. The decay curve for Kr ions lies close to that for Xe ions although it was not plotted. LET of He, N, Ar, and Xe ions were 0.49, 2.91, 8.42, and 16.2 MeV cm^2/mg, respectively. The ranges of these ions were 12.8, 7.36, 7.17, and 8.17 mg/cm^2, using the table data[15] and the additivity rule. Figure 5(a) shows that the initial decay is enhanced with increasing LET, namely, with increasing concentrations of F and H centers and STE's. By contrast, after a few tens

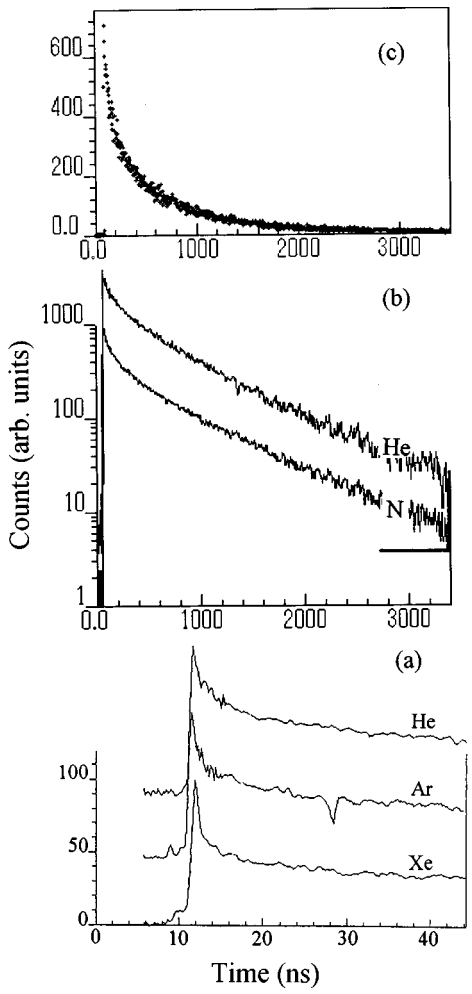

FIG. 5. Projectile-ion-dependent decay of STE luminescence of BaF_2 at room temperature. (a) 2 MeV/nucleon He, Ar, and 1.5 MeV/nucleon Xe ions; (b) 2 MeV/nucleon He and N ions, on log scale; (c) He-ion irradiation, in a wide time range.

of ns, all the decay curves have nearly equal curvatures. This is shown also clearly in Fig. 5(b), which is a log plot of the decay curve over a wide range for N and He ions. Straight lines fitted to the tail parts of the decay curves give the same decay time of 850 ns independent of kinds of ions, being similar to those by the photon and electron irradiation. This means that the decay rate of the tail part is independent of the initial excitation density. Thus, the major excitation-density effect characteristic to the ion irradiation is in the initial decay, but disappears after a short time range of a few tens ns. Figure 5(c) shows a decay curve by He-ion irradiation in much larger range which was measured in a TAC range of 8 μs.

C. Temperature enhanced STE decay

As expressed in the previous sections, it is clear that the regeneration of the STE through the recombination of F and H centers is included in the apparent decay curves of the STE observed. Next, the irradiation temperatures were decreased in order to suppress this regeneration which is sensitive to temperature. Figure 6 gives temperature dependence of He-ion-induced STE decay observed at the temperatures, 298, 100, 60, 40, and 35 K, where the decay curves are

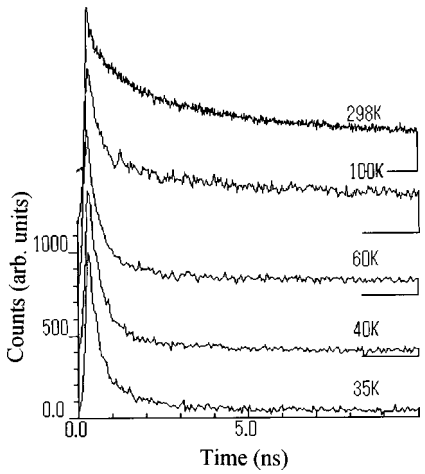

FIG. 6. Temperature-dependent decay of STE luminescence from 2.0 MeV/nucleon He-ion-irradiated BaF_2. Lateral bars at ends of curves show base lines of the respective curves.

plotted in an equal height and with an equal shift of the baseline. The figure shows that the decay was enhanced with decreasing the irradiation temperature. Furthermore, the decay enhancement was prominent in a short time range up to a few ns after the incidence of an ion, and at 35 K it attained an ultimate half lifetime of about 150 ps, which will be shown again in Fig. 8. It is noted that the F, H centers and STE are frozen at this temperature as described in Sec. III A. Such a decay enhancement is contrary to the results known so far for the decay of the STE by photon[6,16] or electron[5] irradiation, which will be mentioned again at the end of this section. On the contrary, as for the tail parts of the decays, the decay times of the tail parts after 5 ns rather increased from 23 to 78 ns with decreasing temperature from 298 to 35 K. This is the same tendency as was the case of photon and electron irradiation. Thus, the temperature effect characteristic in the ion irradiation is also concentrated in the initial stage of the decay here.

Therefore, the decay curves for He, N, Ar, and Kr ions were measured in a narrow TAC range of 20 ns at several temperatures in order to observe the detail of initial decay. Figures 7(a)–7(d) show the decay curves in a range from 0 to 4 ns, where only two decay curves were plotted in each figure since the temperature effect was gradual. Solid lines in the figures are theoretical curves that are described in the Discussion. Figure 7(a) for He-ion irradiation shows that the decrease in temperature from room temperature to 35 K reduced a half lifetime from 1200 to 150 ps and also reduced the intensity of a part of the tail. Similar enhancement in the initial decay was observed also in the case of heavier ion irradiation as shown in Figs. 7(b) to 7(d). An ultimate half lifetime of 150 ps was obtained independent of ion mass (it is noted that the same ultimate half lifetime cannot be ascribed to the resolution of our SISP, since the resolution is enough to measure a half lifetime of 85 ps for the AFL of CsBr). In this case, the increasing excitation density or the increasing LET effect reduces scarcely the tail part of the decay curve, being different from the effect of decreasing temperature by which the recombination of the F-H centers is suppressed.

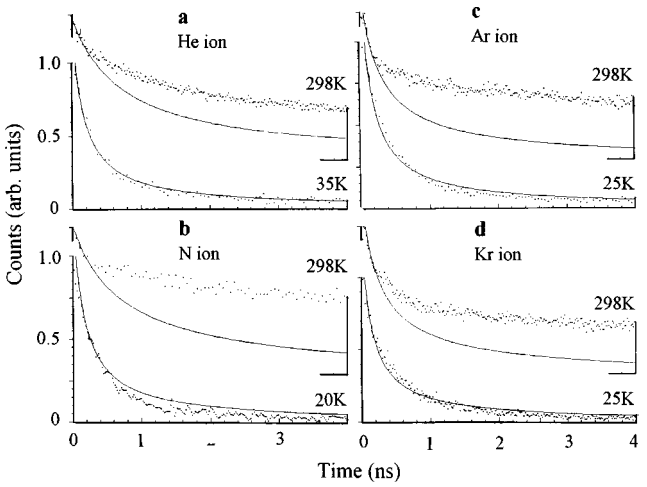

FIG. 7. Projectile-ion and temperature dependence of decay in the initial stage of STE luminescence. Solid lines stand for decay curves calculated by Eq. (A5). Values of **a** were 3.5×10^5 and 1.25×10^6, at room and the lowest temperature for He ions; 3.5×10^5 and 1.2×10^6, for N ions; 7.5×10^4 and 1.25×10^6, for Ar ions; 7.5×10^4 and 1.35×10^6, for Kr ions. The value of 2×10^{-3} ns^{-1} for k_1 was common. The experimental and theoretical peak intensity at time 0 for each ion was equalized to 1.

Next, in order to observe the two effects of the temperature and the ion comprehensively, the relations between luminescence efficiency and half lifetime obtained using various ions at several temperatures are plotted in Fig. 8. Upper and lower insets show the LET dependence of the half lifetime and the luminescence efficiency, respectively. The luminescence efficiency was defined as the luminescence intensity integrated from the peak position to the half lifetime normalized for the ion count (the luminescence efficiency belonging to a time range of the initial decays was remarked consequently). The figure shows that both the luminescence efficiency and the half lifetime are decreased with the increasing LET and also with decreasing temperature; the half lifetime attained an ultimate value, 150 ps. Also, both the LET and temperature effects were varied on nearly the same

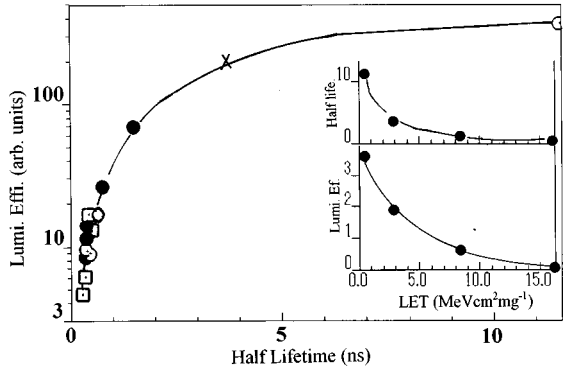

FIG. 8. The luminescence efficiency and half lifetimes with the variation of the ion and the temperatures. The symbol ○ denotes He-ion irradiation at 293, 100, 50, and 40 K, in the order of decreasing half lifetimes; ×, N ions at 293 K; ●, Ar ions, 293, 156, 79, 40, and 25 K; □, Kr ions, 293, 80, 45, and 25 K. The upper and lower insets show the LET dependence of the half lifetime and of the luminescence efficiency, respectively.

curve. Namely, the luminescence efficiency may be expressed by an unique function of the decay rate which is given by the temperature and excitation density. As shown in the insets, both the half lifetime and the luminescence efficiency decreased super linearly to an increase in LET. The super linearity suggests the LET effects should be expressed by more than the first order for the STE concentration, that is, the STE-STE interaction.

The ultimate half lifetime of 150 ps is shorter by one order than the shortest one among the decay times of STE's reported in alkali halides. Such a fast decay cannot be ascribed to the spontaneous decay of the STE, but may be possible only if the STE-STE interaction occurs because of its dense formation. Although there may be interaction between the STE and the F or H center, the temperature effect cannot justify such interactions. It will be discussed further in the Discussion that the STE-STE interaction enhances the STE decay.

Now, two papers are quoted to see the temperature effect on the decay of the STE by photons[6,16] or electrons.[5] According to Shi *et al.*,[6] the decay time of STE luminescence increases from about 1 to 25 μs with decreasing temperatures from room temperature to near 10 K (it is unknown how the time-retarded peak is changed with a decrease in temperature, since the decay curves are not given at lower temperatures than room temperature). The result for electron irradiation by Williams *et al.*[5] is the same at the point that the decay time increases with decreasing temperature. At 10 K, their curve was found to fit to a curve composed of five exponentials, of which the fastest component had a decay time of 12 ns. There can be recognized no time-retarded peak reported by Shi *et al.* and Shibata at room temperature. The decay component of 12 ns had not been assigned decisively there and we also cannot assign it to the net STE decay constant after the recombination of the F-H centers was frozen. The slow down of the STE decay with decreasing temperature may be understood easily by ascribing it to the slow down of the STE regeneration because of the slowdown of the diffusion rate of the F and H centers. In case of the ion irradiation, the temperature dependence at the tail part of the decay presented the same tendency as the photon irradiation, but that of the initial decay was contrary. This can be rather regarded as a phenomenon which cannot be observed by the photon and electron irradiation, considering that its half lifetime is as short as 150 ps. We will try to explain the phenomenon by the STE-STE interaction in Sec. IV C.

IV. DISCUSSION

A. Decay of STE formed at low density at room temperature

A decay curve of photon- or electron-induced STE's, which is at low density, has a rise toward a peak at about 83 or 44 ns after the irradiation pulse, respectively. Let us consider the origin of this rise. As described in the Results, the STE decay may be expressed by following competition between the spontaneous decay and time-retarded regeneration:

$$S \xrightarrow{k_1} h\nu, \tag{1}$$

$$F+H \xrightarrow{k_2} S, \tag{2}$$

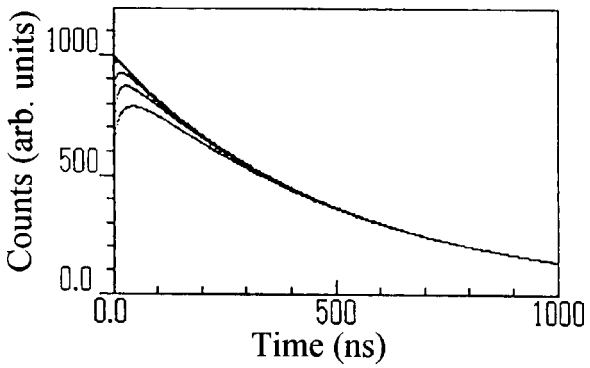

FIG. 9. Theoretical STE decay curves with variation of k_2F_0. Calculations were made by Eq. (4). Values of k_2F_0 were 0.05, 0.15, 0.5, and 3.5 upward, where k_1 and S_0/F_0 were fixed to 0.002 ns^{-1} and 1.0; the uppermost curve is an exponential due to the first term of Eq. (4).

where S stands for the instantaneous concentration of STE. Since F is approximately equal to H, the rate equation due to process (2), reduced to $dF/dt=-k_2F^2/2$, can be solved independently resulting in the solution, $F=F_0/(k_2F_0t+1)$ where F_0 stands for the concentration at time 0. Consequently, a master rate equation for S is given by

$$\frac{dS}{dt}=-k_1S+\frac{k_2}{2}\left(\frac{F_0}{k_2F_0t+1}\right)^2. \tag{3}$$

This equation can be solved analytically and its solution is

$$\begin{aligned} S=&(F_0/2+S_0)\exp(-k_1t)-\frac{F_0}{2(k_2F_0t+1)}\\ &+\frac{k_1}{2k_2}\exp(-A)(E_i(A)-\gamma),\\ A=&k_1\left(t+\frac{1}{k_2F_0}\right), \end{aligned} \tag{4}$$

where E_i stands for an exponential integral and γ is Euler's constant. Luminescence intensity at a given time is proportional to S given in Eq. (4). Equation (4) was compared with the experimental results obtained by photon and electron irradiation given in Fig. 4. The experimental curve was read using a digital scanner and normalized such that the maximum is 1000. The S of Eq. (4) can form a peak if parameters have appropriate values. The best fit curve which has the peak at 44 or 83 ns was obtained as shown in Fig. 4, with the following parameters: In case of photon irradiation, it was when k_1 and k_2F_0 were 0.002 ns^{-1} and 0.02, resulting in $S_0/F_0=1.1$. For electron irradiation, using the same k_1, we obtained $k_2F_0=0.01$, resulting in $S_0/F_0=1.7$. It may rationalize the competing process between Eqs. (1) and (2) that the calculated curves could simulate the experimental ones, especially the peaks.

Although Eq. (4) cannot be applied to the ion-induced decay, it is useful still to know dependence of the function S on k_2 and F_0. Figure 9 shows how the decay curve of the S is varied when k_2F_0 is varied from 0.05 to 3.5 under fixed k_1 of 0.002 ns^{-1} and S_0/F_0 of 1.0. The S has the character that with increasing k_2F_0, its peak shifts asymptotically towards the time 0 with sharpening, but the decay rate cannot exceed that by the first exponential term due to the spontaneous process (1).

B. STE decay under high-density excitation at room temperature

In contrast with sparse formations of STE's by photon and electron irradiation, ion irradiation forms STE's and F-H pairs at extremely high density.[8,9,14] At first, let us discuss the effect of the high density of F-H pairs. Under this condition, geminate F-H pairs can exist no longer isolatedly but overlap with each other, being quite different from the cases of photon and electron irradiation where geminate F-H pairs are isolated. This makes the process (2) much faster because of an increase in F_0. According to Fig. 9, with increasing F_0, the peak of S shifts toward the time 0 with sharpening, and at last the peak of S becomes coincident with that of the first exponential term in Eq. (4) asymptotically. This can explain the result that the STE decay curve for the ion irradiation has no time-retarded peak. However, this process cannot explain the fast initial decay shown in Figs. 5–7, because the fastest decay curve given by the competition between Eqs. (1) and (2) is nothing but an exponential due to the spontaneous decay of the STE. The decay time is at least 12 ns if one assumes the fastest component given by Williams *et al.*[5] The values given by Shi *et al.*[6] and Shibata[7] are 1 μs and 600 ns, respectively. By contrast, the half lifetimes obtained by the ion irradiation are as short as 150 ps in the case of Kr irradiation and the curve is not an exponential. This means that the STE decay in the case of ion irradiation cannot be expressed by the spontaneous decay but must be enhanced much more. Considering the above decay nature, the dense formation of the STE, and the superlinear effect of the STE concentration, it may be reasonable to introduce the nonradiative STE-STE interaction in addition to the competition between Eqs. (1) and (2). Although a competition rate equation composed of above three processes could not be solved analytically, we could solve the competition rate equation in the case where process (2) is eliminated by freezing of the F and H recombination. The STE-STE interaction will be discussed in the next section.

C. Temperature dependence of STE decay

By the discussion given so far, the temperature effect on the tail part of the decay curve, where the density effect is decreased, can be understood easily. It is a natural result that a decrease in temperature reduces the rate of the F and H recombination and hence the rate of the apparent STE decay is reduced through the suppression of their translational and rotational motion. The tail part is therefore similar to the case of photon and electron irradiation. Thus, the temperature effects characteristic in the ion irradiation exist in the initial stage of the STE decay, as was the effect of the excitation density. Therefore, our major interest is in the initial decay.

Now let us consider the system at 30 K where we can neglect the contribution of the F-H recombination to the STE decay. The half lifetime obtained at this temperature was 150 ps. This value is faster at least by one order than that due to the spontaneous decay of the STE of alkali halides known so far. Compared with those for BaF_2, this is faster by the order

of two, even if the fastest component by Williams[5] is taken. It will be discussed later why the elimination of the F-H recombination can enhance the STE decay. We will discuss the resultant decay enhancement. Anyway, such a decay enhancement may be ascribed to the STE-STE interaction by considering the discussion made in the last section. In addition, the interaction must be the one capable to occur without contact, since the STE cannot diffuse at this temperature. Now, there are two types of the distant interactions, one of which is the Dexter-type exchange interaction[17] and the other is the Foerster-type dipolar interaction.[18] The present STE's which may be ascribed to triplet states because of a long lifetime (although a definite value has not yet been obtained) may pertain to the Dexter-type exchange interaction rather than the Foerster-type dipolar interaction. Furthermore, this interaction should be a nonradiative process in the present case, since the luminescence efficiency decreases superlinearly with increasing LET. Consequently, at the lowest temperature, the decay of the STE may be expressed by the competition between process (1) and the following process:

$$S+S \xrightarrow{n(R)} \text{nonradiative.} \tag{5}$$

Now, the rate constant $n(R)$ is controlled by the STE-STE distances. The competition rate equation between Eqs. (1) and (5) could be solved analytically as shown in the Appendix. The resultant solution of S is given by

$$S=\frac{1}{(a+S_0^{-1})\exp(k_1 t)-a}, \tag{A5}$$

where a is a constant relating with a critical distance for the exchange interaction, an effective Bohr radius of the STE, and a track radius R_v, as defined in Eq. (A6). The former two are dependent only on a sample. Then, the a is responsible just for the track radius and hence is related with the STE concentration ($=3S_0/4\pi R_v{}^3$ at $t=0$). It was tried to simulate the experimental decay curves using Eq. (A5) with variations of the a. Both the experimental data at time 0 and S_0 in Eq. (A5) were normalized to 1, because we have no absolute luminescence efficiency. The result was shown by solid lines in Figs. 7(a)–7(d). The figures show that the good fitting could be obtained near 30 K with values of the a given in the caption of Figs. 7(a)–7(d). The figures show also that Eq. (A5) cannot fit the decay curves at higher temperature. This discrepancy is natural since the F-H recombination takes part in the competition at higher temperatures, but these plots may show that the solution is unique for the a. The resultant a was independent of the kind of projectile ions, although this may be expected from the same ultimate half lifetime obtained by the experiment. Nevertheless, it is a surprising result that the ion irradiation from He to Kr ions gives the same initial concentration of STE's in the track. Its meaning will be further discussed later, and next the temperature effect observed will be discussed.

At higher temperature than about 30 K, the competition is composed of processes (1), (2), and (5). Although we could not obtain an analytical solution for this competition rate equation, the decay enhancement observed with decreasing temperature may be interpreted qualitatively. Since the processes of Eqs. (1) and (5) have only small temperature dependence evidently compared with the diffusion of the centers, they can proceed without a large decrease in the rate from room temperature to 30 K, and hence temperature has little influence on the STE decay rate. By contrast, with decreasing temperature, the process of Eq. (2) should be decreased not only in its rate but also in its contribution to the competition. The contribution becomes negligible near 30 K. The fast STE decay given by processes (1) and (5) becomes conspicuous or is bared with decreasing temperature so that the initial decay looks apparently as if it were enhanced. This mechanism may be consistent with the decrease in the luminescence efficiency.

At last, let us discuss the result that the initial concentration of the STE is constant despite that the deposition energy increases by 32 times from He to Xe ions. This may be possible if there are some limiting processes to the STE concentration, which occur at a stage before the formation of the STE because the processes have no influence on the STE decay rate. The initial STE's originate from self-trapping of free excitons and from the electron-hole recombination including recombination of F-H formed in contact. Of these two, free exciton-free exciton reactions seem to be the limiting process by considering as follows. The free exciton is mobile but has a very short lifetime, analogous to the knowledge for alkali halides: the lifetime is believed to be less than sub ps. Therefore, one can assume the critical concentration or the critical distance in order that the free exciton can react with the other free exciton within their lifetimes. If it is supposed that the reaction inhibits the relaxation to the STE, the free excitons which could escape the reaction can relax into the STE. The present result of the same initial concentration of STE's may be interpreted by a tentative mechanism that the concentration of the free exciton formed by the present five ions exceeds the critical one so that the observable effect is only one coming from the critical concentration. This mechanism is consistent with the experimental result that luminescence efficiency at time 0 decreases with increasing LET. Such a reaction of free excitons had been proposed in the case of ion-irradiated KBr by one of the present authors previously:[8(a)] The relative yield at about 5 K of the σ-to-π STE increased with increasing the excitation density but their decay curves were unchanged. This was explained by the interaction between free excitons in an earlier stage than the STE formation.

V. CONCLUSIONS

In contrast to the result for the photon and electron irradiated BaF_2, the ion-induced STE decay does not only present the time-retarded rise but also its rate was extraordinarily faster in the initial stage. The decay enhancement was superlinear with increasing excitation density. The photon- or electron-induced decay curve with a time-retarded peak could be simulated by a competition kinetics between the spontaneous decay of STE's and the regeneration of STE by the recombination of the F and H centers (the V_k centers should be comprised in holes). This recombination should be a reason why BaF_2 is a radiation-protective substance compared with alkali halides. By contrast, in the ion track, the geminate pairs do not exist sparsely but they are overlapped because they are formed at high density, resulting in no ob-

servable time-retarded peak. However, this mechanism cannot explain the ion-induced large enhancement of the STE decay nor the large enhancement caused by decreasing temperature, since the large decay enhancement took place still at 30 K where both the centers and the STE are frozen. The STE-STE exchange interaction was proposed as nonradiative and distant interaction. A competition rate equation between the spontaneous decay and the exchange interaction was assumed at 30 K and solved analytically. The result could simulate the experimental decay. The unusual decay enhancement observed at the initial stage with decreasing temperature, was explained by a mechanism that the exchange interaction became prominent as a result of the suppression of the time-retarded STE regeneration. The result that an ultimate half lifetime of about 150 ps was obtained independently of projectile ions of He, N, Ar, Kr, and Xe means that the density of STE's in the incipient track is nearly the same among tracks formed by these ions. This may be explained tentatively by the mechanism that in the incipient track, there occurs vigorous interaction between the precursors of STE's such as free excitons so that the concentration of the surviving free excitons is limited to the critical concentration. The existence of the interaction in the stage of precursors of STE's is similar to the result found for ion-irradiated alkali-halide single crystals by the present authors.[8(a)] Tanimura and Itoh have reported a transient luminescence spectrum in laser-irradiated RbI which they assigned to a complex between a free exciton and a STE.[19] Although we could not recognize such a spectrum in the present system, it may be interesting to study on such complexes in many other ionic crystals using ion irradiation because ion irradiation can excite them at extremely high density.

ACKNOWLEDGMENTS

The authors are indebted to Professor S. Kazama of Chuo University and many former students of his laboratory. Also, they acknowledge Professor N. Itoh and Dr. A. Kira for their helpful discussions.

APPENDIX

When STE decays under the competition between processes (1) and (5), the corresponding rate equation is described and solved here. The average number of STE's formed in each ion track is represented as S and STE's were supposed to be homogeneously distributed. This assumption seems not to be so far from the reality, because the 2-MeV/nucleon ion forms the track composed mostly of the core part, being different from the track comprising a large part of the hollow part (see also Sec. III B). Also, STE disappears pairwise with a rate-constant dependent on a separation distance R of the pair and does not make diffusion. The number of STE's which exists in the distance from R to $R+dR$ can be described as $2\pi SR^2dR/V$, where V stands for the volume of one track. The rate of the exchange interaction at the distance R can be expressed as $2\pi n(R)S^2R^2dR/V$ where $n(R)$ is the rate constant of the exchange interaction at the distance R. The $n(R)$ is given by Dexter[17] and Inokuti and Hirayama[20] as follows:

$$n(R)=k_1\ \exp\left\{\delta\left(1-\frac{R}{R_0}\right)\right\},$$
$$\delta=\frac{2R_0}{L}, \tag{A1}$$

where L is the effective average Bohr radius of the STE, R_0 is the distance where both rates through the spontaneous decay and the exchange interaction are equal. The rate of the exchange interaction can be obtained by the summation of all the rates corresponding to every distance. A resultant master rate equation is given by the following:

$$\frac{dS}{dt}=-k_1S-\int_0^{R_v}n(R)\ \frac{2\pi S^2R^2dR}{V}, \tag{A2}$$

where R_v is the track radius. If we set

$$a=k_1^{-1}\int_0^{R_v}n(R)\ \frac{2\pi R^2}{V}\,dR, \tag{A3}$$

then Eq. (A2) can be reduced to a simple differential equation

$$\frac{dS}{dt}=-k_1(S+aS^2). \tag{A4}$$

The solution of Eq. (A4) is given by

$$S=\frac{1}{(a+S_0^{-1})\exp(k_1t)-a}, \tag{A5}$$

where S_0 is the number of STE at time 0. The luminescence at time t is proportional to the S. By assuming the volume V as a sphere with radius ($V=4\pi R_v^3/3$), the integral in Eq. (3) can be calculated to give

$$a=\frac{3}{2}\exp(\delta)[2\xi^3-\{\xi+2\xi^2+2\xi^3\}\exp(\xi)],$$
$$\xi=\frac{R_0}{R_v\delta}=\frac{L}{2R_v}. \tag{A6}$$

[1] M. Laval, M. Moszynsky, R. Allemeand, E. Cormoreche, P. Guinet, R. Odru, and J. Vacher, Nucl. Instrum. Methods Phys. Res. **206**, 169 (1983).

[2] Yu. M. Aleksandrov, V. N. Makhov, P, A. Rodonyi, T. TI. Syreishchikova, and V. N. Yakimenko, Sov. Phys. Solid State **26**, 1734 (1984).

[3] S. Kubota, M. Itoh, Jian-zhi Ruan(Gen), S. Sakuragi, and S. Hashimoto, Phys. Rev. Lett. **60**, 2319 (1988); S. Kubota, J. Ruan, M. Itoh, S. Hashimoto, and S. Sakuragi, Nucl. Instrum. Methods Phys. Res. A **289**, 253 (1990).

[4] J. H. Beaumont, W. Hayes, D. L. Kirk, and G. P. Summers, Proc. R. Soc. London, Ser. A **315**, 69 (1970).

[5] R. T. Williams, M. N. Kabler, W. Hayes, and J. P. Stott, Phys. Rev. B **14**, 725 (1976).

[6] C. Shi, T. Kloiber, and G. Zimmerer, Phys. Scr. **41**, 1022 (1990); J. Lumin. **48**, 597 (1991).
[7] H. Shibata (private communication).
[8] K. Kimura and J. Wada, Phys. Rev. B **48**, 15 535 (1993).
[9] (a) K. Kimura, K. Mochizuki, T. Fujisawa, and M. Imamura, Phys. Lett. **78A**, 108 (1980); (b) K. Kimura, T. Matsuyama, and H. Kumagai, Radiat. Phys. Chem. **34**, 575 (1989); (c) K. Kimura and H. Kumagai, Radiat. Eff. Defects Solids **126**, 45 (1992); (d) K. Kimura, Nucl. Instrum. Methods Phys. Res. B **90**, 100 (1994).
[10] A computer program was made according to J. F. Ziegler, *Stopping Cross Sections for Energetic Ions in All Elements* (Pergamon, New York, 1977), Vol. 1–5.
[11] Absorption bands due to color centers were not recognized at room temperature by a dose higher by one order than that used in this experiment, although at 77 K, F centers were recognized. The STE luminescence intensity at time 0 of its decay curve was the highest near room temperature. They will be published elsewhere.
[12] R. B. Murray and A. Meyer, Phys. Rev. **122**, 815 (1961); A. Meyer and R. B. Murray, *ibid.* **128**, 98 (1962).
[13] F. D. Becchetti, C. E. Thorn, and M. J. Levin, Nucl. Instrum. Methods **138**, 93 (1976).
[14] K. Kimura, Phys. Rev. A **47**, 327 (1993).
[15] L. C. Northcliffe and R. F. Schilling, *Nuclear Data Tables* (Academic, New York, 1970).
[16] A. V. Agafonov and P. A. Rodnyi, Sov. Phys. Solid State **25**, 335 (1983).
[17] D. J. Dexter, J. Chem. Phys. **21**, 836 (1953).
[18] Th. Foerster, Ann. Phys. (Leipzig) **2**, 55 (1948).
[19] K. Tanimura and N. Itoh, Phys. Rev. Lett. **60**, 2753 (1988); **64**, 1429 (1989).
[20] M. Inokuti and F. Hirayama, J. Chem. Phys. **43**, 1978 (1965).